

tion. Ideally, the charge capacity of the two electrochromic films should be equal, and the capacity of the device should be the sum of film capacities. The LBL technique can be used to vary the number of layers, and composition of each layer, to improve charge capacity. The amount of PEDOT contained in each layer can also be increased to balance charge in the layers.

In summary, working electrochromic devices have been constructed for the first time with two complementary chromic LBL polymer systems. Initial results are promising, indicating that highly stable, uniform films can be produced which switch between colored and bleached states in under 2 s. The cells have been shown to undergo over 35 000 cycles without failure utilizing a PAMPS/H₂O ion transport medium. These results introduce a viable and potentially lucrative electrochromic device fabrication method to the field, which can be applied to a number of electrochromic materials. The speed and high stability of the devices make them good candidates for smart windows or large area, long term displays. The contrast in these devices is not optimal, particularly in comparison with newly designed polyelectrochromes which can achieve close to 60 % contrast;^[6] however, by changing the electrochromic polyion and fine-tuning the bilayer number, co-polyion, and deposition conditions, we expect that such performance can be achieved in these LBL devices. In addition, we are currently investigating different forms of solid polymer electrolytes, including other polymer LBL systems, to create a completely LBL assembled device. The many variables available to LBL assembly ensure that quick progress can be achieved in optimizing color contrast, switching speed, and the long-term stability of these new electrochromic systems.

Experimental

Polymers included PANI (Aldrich), LPEI (Polysciences), PAMPS (Aldrich), and PEDOT:SPS (BAYTRON P, Bayer Corporation). Polymer solutions were made using Milli-Q (Millipore) water. PANI and PEDOT:SPS solutions were prepared with an aqueous co-solvent including dimethylacetamide at 10 mM polymer as described by Rubner [13] (polymer concentrations with respect to repeat unit). LPEI solutions were 20 mM. PAMPS solutions were 2 mM. ITO-glass substrates were cleaned by ultrasonication in surfactant solution and Milli-Q water, followed by a 5 min oxygen plasma etch (Harrick PCD 32G). Gold milli-electrodes were prepared by evaporating 99.99 % gold shot (American Metals) through a shadow mask onto polyolefin plates. Film assembly was automated with a modified Carl Zeiss HMS DS-50 slide stainer. The substrates were dipped in polycation solution for 15 min, rinsed for 4 min in Milli-Q, and then dipped in polyanion solution for 15 min and then rinsed again. This cycle was repeated 20 times for 20 bilayers. Polymer electrolyte was prepared by casting PAMPS from aqueous solution. PAMPS films were equilibrated at 65 % relative humidity (RH). Electrodes were then pressure laminated. Devices were stored at 65 % RH. Film thickness was measured by Tencor profilometer. CV and chronocoulometry were performed using an EG&G 263A potentiostat/galvanostat. For (PANI/PAMPS)₂₀, the electrolyte was 0.1 M H₂SO₄. For (LPEI/PEDOT)₂₀ films, the electrolyte was 0.1 M NH₄Cl. Counter electrode was 4 cm² platinum foil and reference was K-SCE. Spectral characterization of the individual films was performed with an HP spectrophotometer and a BAS potentiostat. ITO substrates were positioned in a quartz cell with electrolyte, platinum coil working electrode, and SCE. Assembled devices were electrically characterized using the EG&G 263A with a sense electrode. Devices were optically characterized using an Oriel UV-vis spectrophotometer with a 1200 L/mm, 300 nm blaze Oriel grating and InstaSpec IV charge coupled device (CCD), with grating angle adjusted manually for full range.

Received: March 15, 2001
Final version: May 25, 2001

- [1] R. Dagani, *Chem. Eng. News* **2001**, 79, 40.
- [2] A. Seeboth, J. Schneider, A. Patzak, *Sol. Energy Mater. Sol. Cells* **2000**, 60, 263.
- [3] M. Green, *Chem. Ind.* **1996**, 17, 641.
- [4] P. M. S. Monk, R. J. Mortimer, D. R. Rosseinsky, *Electrochromism: Fundamentals and Applications*, VCH, Weinheim, **1995**.
- [5] R. J. Mortimer, *Electrochim. Acta* **1999**, 44, 2971.
- [6] S. A. Sapp, G. A. Sotzing, J. R. Reynolds, *Chem. Mater.* **1998**, 10, 2101.
- [7] R. D. Rauh, F. Wang, J. R. Reynolds, D. L. Meeker, *Electrochim. Acta* **2001**, 46, 2023.
- [8] I. D. Brotherston, D. S. K. Mudigonda, J. M. Osborn, J. Belk, J. Chen, D. C. Loveday, J. L. Boehme, J. P. Ferraris, D. L. Meeker, *Electrochim. Acta* **1999**, 44, 2993.
- [9] D. S. K. Mudigonda, J. L. Boehme, I. D. Brotherston, D. L. Meeker, J. P. Ferraris, *Chem. Mater.* **2000**, 12, 1508.
- [10] G. Decher, J. D. Hong, *Makromol. Chem. Macromol. Symp.* **1991**, 46, 321.
- [11] F. Rubner, J. H. Cheung, A. F. Fou, *Thin Solid Films* **1994**, 244, 985.
- [12] M. F. Rubner, M. Ferreira, J. H. Cheung, *Thin Solid Films* **1994**, 244, 806.
- [13] M. F. Rubner, J. H. Cheung, W. B. Stockton, *Macromolecules* **1997**, 30, 2712.
- [14] M. F. Rubner, W. B. Stockton, *Macromolecules* **1997**, 30, 2717.
- [15] J. B. Schlenoff, D. Laurent, *Langmuir* **1997**, 13, 1552.
- [16] J. B. Schlenoff, J. Stepp, *J. Electrochem. Soc.* **1997**, 144, L155.
- [17] J. B. Schlenoff, H. Ly, M. Li, *J. Am. Chem. Soc.* **1998**, 120, 7626.
- [18] J. B. Schlenoff, S. T. Dubas, T. Farhat, *Langmuir* **2000**, 16, 9968.
- [19] S. T. Dubas, J. B. Schlenoff, *Macromolecules* **1999**, 32, 8153.
- [20] P. T. Hammond, G. M. Whitesides, *Macromolecules* **1995**, 28, 7569.
- [21] S. L. Clark, M. F. Montague, P. T. Hammond, *Supramol. Sci.* **1997**, 4, 141.
- [22] S. L. Clark, M. F. Montague, P. T. Hammond, *Macromolecules* **1997**, 30, 7237.
- [23] X. Jiang, P. T. Hammond, *Langmuir* **2000**, 16, 8501.
- [24] R. D. Giglia, G. Haacke, in *Performance Improvements In WO₃-Based Electrochromic Displays*, Vol. IS 4 (Eds: C. M. Lampert, C. G. Granqvist), SPIE, Hamburg **1988**, pp. 41–45.
- [25] M.-C. Bernard, A. H.-L. Goff, W. Zeng, *Electrochim. Acta* **1998**, 44, 781.
- [26] Q. Pei, G. Zuccarello, M. Ahlskog, O. Inganäs, *Polymer* **1994**, 35, 1347.
- [27] T. Kobayashi, H. Yoneyama, H. Tamura, *J. Electroanal. Chem.* **1984**, 161, 419.
- [28] A. G. MacDiarmid, B. D. Humphrey, W.-S. Huang, *J. Chem. Soc., Faraday Trans. 1* **1986**, 82, 2385.

Emulsion Templating Using High Internal Phase Supercritical Fluid Emulsions**

By Rachel Butler, Cait M. Davies, and Andrew I. Cooper*

Emulsion templating is a versatile method for the preparation of well-defined porous polymers^[1] and inorganic materials.^[2] In general, the technique involves forming a high internal phase emulsion (HIPE) (>74.05 % v/v internal phase) and locking in the structure of the “external” phase, usually by reaction induced phase separation (e.g., sol–gel chemistry, free-radical polymerization). Subsequent removal of the internal phase (i.e., the emulsion droplets) gives rise to a skeletal replica of the emulsion. In principle, templated oil-in-water (O/W) emulsions provide a direct synthetic route to a variety

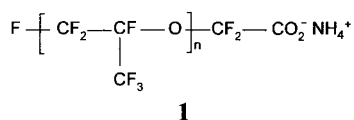
[*] Dr. A. I. Cooper, R. Butler, C. M. Davies
Donnan and Robert Robinson Laboratories, Department of Chemistry
University of Liverpool
Crown Street, Liverpool L69 3BX (UK)
E-mail: aicooper@liv.ac.uk

[**] The authors acknowledge The Royal Society for a University Research Fellowship (to AIC), Bradford Particle Design plc for a CASE Award (to RB), and the Engineering and Physical Sciences Research Council (EPSRC) for financial support.

of porous hydrophilic polymers for applications such as separation media, catalyst supports, biological tissue scaffolds, and controlled release devices. However, O/W techniques are extremely solvent intensive because the internal oil phase (often an organic solvent) can constitute between 75 and 90 % of the total reaction volume. Furthermore, it may be very difficult to remove the template from the material at the end of the reaction. For inorganic materials, purification tends to involve firing the sample at high temperatures (>600 °C), thus completely removing any organic residues.^[2] This is clearly not practical for organic polymers or inorganic–organic hybrid materials that decompose at relatively low temperatures. In such cases, complete removal of the template may be much more problematic, particularly in applications where solvent residues are undesirable (e.g., biomedical devices). In this communication, we show that these problems can be overcome by templating supercritical CO₂-in-water (C/W) emulsions. Together, water and CO₂ are two of the most abundant and environmentally benign solvents on Earth. Entrapment of the template phase is completely avoided because CO₂ reverts to the gaseous state upon depressurization.

Supercritical carbon dioxide (scCO₂) has been promoted recently as a sustainable solvent because it is non-toxic, non-flammable, and naturally abundant.^[3] In particular, scCO₂ has been shown to be a versatile solvent for polymer synthesis and processing.^[4] A number of research groups have exploited carbon dioxide for the preparation of porous polymers. For example, scCO₂ has been used for the production of microcellular polymer foams,^[5] biodegradable composite materials,^[6] macroporous polyacrylates,^[7] and fluorinated microcellular materials.^[8] All of these supercritical fluid (SCF) techniques involve either a foaming mechanism,^[5,6] gelation of the SCF medium (i.e., an organic equivalent of sol–gel chemistry),^[7,8] or a combination of both.^[8] This limits the range of porous materials which can be accessed via the scCO₂ route because many materials cannot be foamed or derived from CO₂-soluble precursors. We present here an entirely new approach to the synthesis of porous materials which involves templating high internal phase SCF emulsions. The technique has wide appeal because it allows the synthesis of materials with well-defined porous structures without the use of any volatile organic solvents—just water and CO₂.

Our methodology was inspired by Johnston's recent studies on the formation and stability of water-in-CO₂ (W/C) and C/W emulsions.^[9–11] Many conventional hydrocarbon surfactants used in O/W systems exhibit low solubilities in CO₂ and are incapable of forming W/C or C/W emulsions.^[12] By contrast, surfactants with fluoroalkyl or fluoroether tails are quite soluble because the weak dispersion forces for these tails are well matched to those of CO₂. Johnston has shown that perfluoropolyether (PFPE) surfactants (i.e., **1**) can form both W/C and C/W macroemulsions, and that these emulsions can exhibit



kinetic stability.^[9] W/C microemulsions have been evaluated in applications such as inorganic^[13] and organic synthesis,^[14] catalysis,^[15] and the manipulation of water-soluble biomolecules.^[16]

The general procedure for templating a C/W emulsion is shown in Figure 1. Our preliminary studies have mostly involved the preparation of cross-linked acrylamide (AM)-based polymers, although the results suggest that the

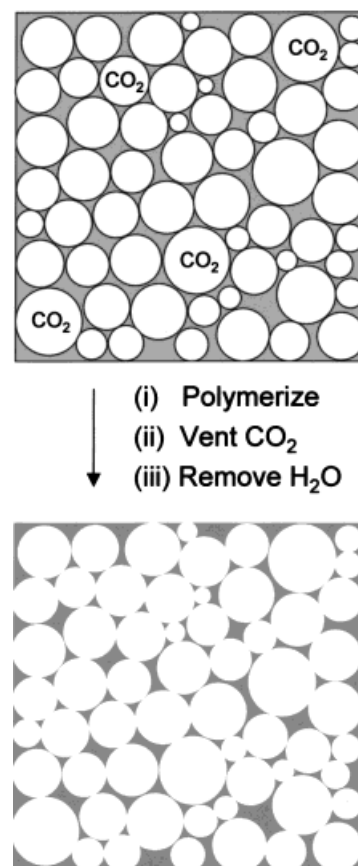


Fig. 1. Preparation of a porous material via SCF emulsion templating. External phase is an aqueous solution, internal droplet phase is scCO₂.

approach might also be applied to a much wider range of materials. We chose to use a relatively low molecular weight PFPE ammonium carboxylate surfactant ($M_w = 567 \text{ g mol}^{-1}$), since Johnston has demonstrated that surfactants of this type exhibit significant solubility in water and have a propensity to form C/W rather than W/C emulsions.^[9]

First of all, we studied the emulsification of pure water and CO₂ (temperature = 25 °C, CO₂ pressure = 100–300 bar, volume fraction of CO₂ = 70 %, surfactant concentration = 1–10 % w/v based on H₂O). Milky-white C/W emulsions were formed which filled the entire reaction vessel. Depending on the precise conditions, the emulsions could be stable for more than 1 h after stirring was ceased, although some degree of settling usually occurred after extended periods (i.e., several hours). These results suggested that this system was suitable for emulsion templating because the free-radical polymerization chemistry would be expected to occur before the emulsion became destabilized.

When pure water was replaced with a 40 % w/v solution of AM and *N,N*-methylene bisacrylamide (MBAM) (AM/MBAM = 8:2 w/w), it was found that the corresponding emulsions were much less stable. In the absence of stirring, rapid separation occurred over a period of a few minutes leading to two distinct phases: a transparent upper phase (CO₂) and a white milky lower phase (H₂O with a small amount of emulsified CO₂). This instability became even more pronounced as the mixture was heated to 60 °C. In the presence of a water-soluble initiator (K₂S₂O₈, 2 % w/v based on monomer), polymerization occurred and gelation of the aqueous phase was observed. The solidified gel occupied somewhat less than 50 % of the reactor volume, suggesting that only a small quantity of CO₂ had been emulsified and “templated”. The sample was dried in vacuum, fractured into small pieces, and studied by scanning electron microscopy (SEM). The electron micrographs confirmed that the templated pores were isolated and exclusively closed-cell in nature. Mercury intrusion porosimetry analysis showed that the degree of porosity was low (0.2–0.5 cm³ g⁻¹).

Clearly, the presence of the organic monomers had caused significant destabilization of the C/W emulsion. This may be because the monomers act as de-emulsifiers by adsorbing at the water–CO₂ interface, thus reducing interfacial tension gradients and hence droplet stability.^[9] It was found that this destabilization could be counteracted by the addition of poly(vinyl alcohol) (PVA) to the aqueous phase prior to polymerization (10 % w/v relative to H₂O, see Table 1). Again, the kinetic stability of the C/W emulsions tended to decrease somewhat with increasing temperature, but in the presence of PVA the systems were sufficiently stable for templating to occur and for open-cell porous materials to be produced (Fig. 2). The materials conformed closely to the interior of the reaction vessel and no significant shrinkage was observed upon venting the CO₂, although some shrinkage always occurred when the polymers were dried.

At a CO₂ phase volume fraction of 70 %, open-cell porous polymers were formed with pore volumes in the range 1.8–2.6 cm³ g⁻¹ and median pore diameters in the range 1.5–5.4 μm (Table 1, samples 1–6). The median pore size as measured by mercury intrusion porosimetry agreed qualitatively with the size of the holes observed in the cell walls between the templated CO₂ emulsion droplets (see Fig. 2). The concentration of surfactant **1** with respect to the aqueous phase was varied over the range 0.25–5 % w/v. Neither the intrusion volume nor the median pore diameter varied greatly as a function of surfactant concentration at this CO₂-to-water phase ratio, although the morphology of the porous structure did vary significantly. In general, higher surfactant concentrations led to more open, interconnected structures with an increased number of interconnecting pores in the cell walls (see Fig. 2a,b). Substitution of AM with 2-hydroxyethyl acrylate (sample 4) also led to porous, open-cell materials, suggesting that this technique might be applied to a wide range of hydrophilic polymers and hydrogel materials.

In an attempt to increase the level of porosity in the samples, the volume fraction of the CO₂ internal phase was

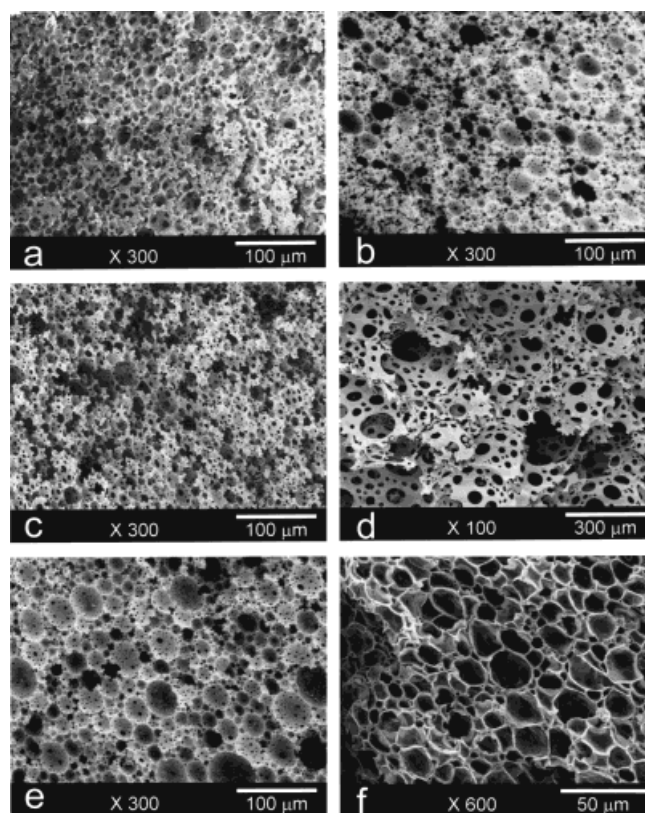


Fig. 2. SEM images of templated porous polymers produced from C/W emulsions. a) Sample 3 (CO₂/H₂O = 70:30 v/v, 1 % w/v surfactant **1** based on H₂O). b) Sample 5 (CO₂/H₂O = 70:30 v/v, 5 % w/v surfactant **1**). c) Sample 7 (CO₂/H₂O = 75:25 v/v, 1 % w/v surfactant **1**). d) Sample 8 (CO₂/H₂O = 80:20 v/v, 1 % w/v surfactant **1**). e) Sample 9 (CO₂/H₂O = 80:20 v/v, 2 % w/v surfactant **1**). f) Sample 11 (CO₂/H₂O = 75:25 v/v, PVA cross-linked with glutaraldehyde, 2 % w/v surfactant **1**, see Table 1).

Table 1. Emulsion templating using C/W emulsions.

	volume fraction CO ₂ [%]	% 1 (w/v based on H ₂ O)	% 1 (w/v based on CO ₂)	V _{pore} [cm ³ g ⁻¹] [a]	median pore diameter [μm] [b]
1	70	0.25	0.11	2.0	3.8
2	70	0.5	0.21	2.6	3.8
3	70	1	0.43	2.1	5.4
4 [c]	70	1	0.43	1.8	1.5
5	70	5	2.14	2.0	1.8
6 [d]	70	5	2.14	2.4	3.1
7	75	1	0.33	1.2	2.3
8	80	1	0.25	5.9	55
9	80	2	0.50	3.9	3.9
10	80	3	0.75	3.8	4.0
11 [e]	75	2	0.66	2.4	7.7

Reaction conditions (samples 1–10): AM + MBAM (40 % w/v in H₂O, AM/MBAM = 8:2), K₂S₂O₈ (2 % w/v), PVA (10 % w/v based on H₂O, 80 % hydrolyzed, M_w = 9–10 kg mol⁻¹), 60 °C, 250–290 bar, 12 h. [a] Total intrusion volume, as measured by mercury intrusion porosimetry over the pore size range 7 nm–100 μm. [b] Measured by mercury intrusion porosimetry. [c] 2-Hydroxyethyl acrylate used in place of AM. [d] AM/MBAM = 9:1 w/w. [e] 20 % w/v PVA based on H₂O, glutaraldehyde (12 % w/w based on PVA), 70 °C, 355 bar, 12 h.

increased from 70 % to 75 % (sample 7) and 80 % (samples 8, 9 + 10). Even under such concentrated conditions, it was possible to form C/W emulsions that filled the entire reaction ves-

sel. Polymerization of these C/W HIPEs led to materials with an even more open, porous structure, and with total pore volumes as high as $5.9 \text{ cm}^3 \text{ g}^{-1}$ (Table 1). Sample 8 exhibited a much larger average pore diameter ($55 \mu\text{m}$) than the other samples (Fig. 2d), probably because the concentration of surfactant **1** was kept constant relative to the external aqueous phase while the volume fraction of the internal CO_2 phase was increased. Thus, the surfactant was required to stabilize an increasingly large interfacial area and the average CO_2 droplet size became correspondingly larger. At this higher CO_2 -to-water phase ratio, it was found that the average cell size and pore diameter decreased significantly when the concentration of surfactant **1** was raised to 2 or 3 % w/v (samples 9 + 10, Fig. 2e). Unlike samples 1–6, samples 7–10 were derived from high internal phase emulsions ($>74.05 \text{ \% v/v}$). As such, the internal phase volume exceeded the close-packed sphere limit. This causes the emulsion droplets to deform into polyhedra and creates a more open structure in the templated material.^[1] The surface area of all samples was measured by nitrogen adsorption/desorption (Brunauer–Emmett–Teller, BET, method) and was found to be relatively low ($<5 \text{ m}^2/\text{g}$). This suggests that these materials did not retain any additional permanent, dry porosity within the walls of the templated structure.

The physical basis for the large increase in emulsion stability caused by the addition of the PVA “cosurfactant” is not yet understood. One possible interpretation is that the PVA causes an increase in the interfacial viscosity and the monolayer bending elasticity, thus inhibiting tangential interfacial flow in the thin aqueous film between the CO_2 droplets.^[9,17] Preliminary experiments suggest that the addition of PVA also enhances the long-term stability of these C/W emulsions in the absence of organic monomers such as acrylamide. Clearly, further work is needed to understand the stabilization of these multicomponent emulsions and to allow the design of more efficient surfactants and cosurfactants.

The C/W emulsion droplets were not monodisperse, as is evident from the distribution of cell sizes observed in the electron micrographs (Fig. 2). This suggests that the technique in its current form may not be suitable for the preparation of highly ordered structures (e.g., photonic band gap materials), although it is possible to synthesize templated polymers with well-defined pore size distributions, as shown in Figure 3. We

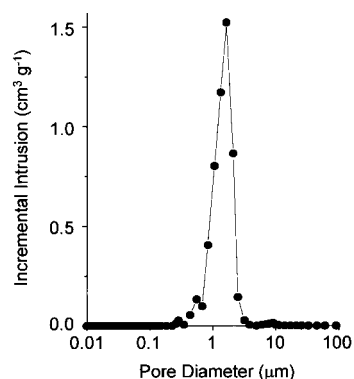


Fig. 3. Mercury intrusion porosimetry data for sample 5. Median pore diameter = $1.8 \mu\text{m}$, total intrusion volume = $2.0 \text{ cm}^3 \text{ g}^{-1}$.

believe that it would be relatively straightforward to adapt our approach to the synthesis of a range of porous structures, including hybrid macroporous/microporous inorganic materials produced by sol–gel routes.^[2] However, perhaps the greatest potential lies in the preparation of hydrophilic organic polymers or inorganic–organic hybrid materials where removal of the internal organic phase cannot be achieved by treatment at high temperatures. Our methodology opens up an entirely new “solvent-free” route for the synthesis of porous biopolymers, hydrogels, and composites, including materials which cannot readily be produced by foaming. For example, preliminary studies have demonstrated that it is possible to produce templated, cross-linked PVA materials by gelation of C/W HIPEs containing PVA and glutaraldehyde in the external aqueous phase (sample 11, Fig. 2f).

In summary, we have developed a new method for producing well-defined porous materials by templating scCO_2 emulsions. In contrast to other O/W templating techniques, our approach does not involve any volatile organic solvents either in the synthesis or in the purification steps. Future work will focus on the extension of this approach to a wider range of materials, and on achieving fine control over porous structure by tuning the CO_2 density. We will also investigate alternative, biodegradable hydrocarbon surfactants for the preparation of templated materials from C/W emulsions.^[18]

Experimental

Materials: Poly(hexafluoropropyleneoxide-co-difluoromethyleneoxide) monocarboxylic acid ($M_w = 554 \text{ g mol}^{-1}$, Aldrich), ammonia solution (BDH Chemicals), AM (99+ %, Aldrich), MBAM (99 %, Aldrich), potassium persulfate (99+ %, Aldrich), PVA ($M_w = 9\text{--}10 \text{ kg mol}^{-1}$, 80 % hydrolyzed, Aldrich), and glutaraldehyde (50 % w/v solution in water, Aldrich) were all used as received.

Synthesis: Surfactant **1** was synthesized according to literature procedures [9]. High pressure reactions were carried out in a stainless steel reactor (10 cm^3), equipped with a sapphire window for observation of phase behavior. In a typical polymerization, the reactor was charged with an aqueous solution of monomers (40 % w/v), initiator ($\text{K}_2\text{S}_2\text{O}_8$, 2 % w/v based on monomer), surfactant **1**, and a cosurfactant (e.g., PVA) before purging with a slow flow of CO_2 for 15 min. The reactor was then pressurized with liquid CO_2 ($20 \pm 2 \text{ }^\circ\text{C}$, $100 \pm 5 \text{ bar}$) and stirring (poly(tetrafluoroethylene), PTFE, stir bar) was commenced, whereupon a white, milky C/W emulsion was formed. For experiments involving cross-linked PVA materials (e.g., sample 11), a motor-driven impeller stirrer (500–1500 rpm) was used to achieve emulsification because of the higher viscosity of the aqueous phase. Stirring was continued for 30 min and then ceased before heating the reactor to the required reaction temperature overnight ($60 \text{ }^\circ\text{C}$, $275 \pm 20 \text{ bar}$). (SAFETY NOTE: The onset of polymerization was sometimes accompanied by a reaction exotherm, which caused a sudden increase in temperature and pressure. An adequately vented safety rupture device is strongly recommended for these experiments). After cooling to room temperature, the CO_2 was vented and the templated polymers were removed from the reactor. Residual water was removed from the samples by drying in air for 24 h followed by drying under vacuum at $50 \text{ }^\circ\text{C}$ overnight.

Characterization: For analysis, the continuous polymer samples were fractured into millimeter-sized pieces with a scalpel. Pore size distributions were recorded by mercury intrusion porosimetry using a Micromeritics Autopore IV 9500 porosimeter. Samples were subjected to a pressure cycle starting at approximately 0.5 psia, increasing to 60 000 psia in predefined steps to give pore size/pore volume information. Polymer surface areas were measured using the BET method with a Micromeritics Tristar nitrogen adsorption analyzer. Samples were outgassed for 3 h at $60 \text{ }^\circ\text{C}$ under a N_2 flow before analysis. Polymer morphologies were investigated with a Hitachi S-2460N SEM. Samples were mounted on aluminum studs using adhesive graphite tape and sputter coated with approximately 10 nm of gold before analysis.

Received: April 2, 2001
Final version: June 5, 2001

- [1] a) N. R. Cameron, D. C. Sherrington, *Adv. Polym. Sci.* **1996**, *126*, 163. b) P. Hainey, I. M. Huxham, B. Rowatt, D. C. Sherrington, L. Tetley, *Macromolecules* **1991**, *24*, 117. c) A. Barbetta, N. R. Cameron, S. J. Cooper, *Chem. Commun.* **2000**, 221. d) N. R. Cameron, A. Barbetta, *J. Mater. Chem.* **2000**, *10*, 2466.
- [2] a) A. Imhof, D. J. Pine, *Adv. Mater.* **1998**, *10*, 697. b) A. Imhof, D. J. Pine, *Nature* **1997**, *389*, 948. c) G.-R. Yi, S.-M. Yang, *Chem. Mater.* **1999**, *11*, 2322. d) V. N. Manoharan, A. Imhof, J. D. Thorne, D. J. Pine, *Adv. Mater.* **2001**, *13*, 447.
- [3] *Chemical Synthesis using Supercritical Fluids* (Eds: P. G. Jessop, W. Leitner), WILEY-VCH, Weinheim **1999**.
- [4] a) J. M. DeSimone, Z. Guan, C. S. Elsbernd, *Science* **1992**, *257*, 945. b) J. M. DeSimone, E. E. Maury, Y. Z. Menceloglu, J. B. McClain, T. J. Romack, J. R. Combes, *Science* **1994**, *265*, 356. c) F. A. Adamsky, E. J. Beckman, *Macromolecules* **1994**, *27*, 312. d) A. I. Cooper, W. P. Hems, A. B. Holmes, *Macromolecules* **1999**, *32*, 2156. e) J. L. Kendall, D. A. Canelas, J. L. Young, J. M. DeSimone, *Chem. Rev.* **1999**, *99*, 543. f) A. I. Cooper, *J. Mater. Chem.* **2000**, *10*, 207. g) A. I. Cooper, *Adv. Mater.* **2001**, *13*, 1111.
- [5] a) S. K. Goel, E. J. Beckman, *Cell. Polym.* **1993**, *12*, 251. b) S. K. Goel, E. J. Beckman, *Polym. Eng. Sci.* **1994**, *34*, 1137. c) K. A. Arora, A. J. Lesser, T. J. McCarthy, *Polym. Eng. Sci.* **1998**, *38*, 2055.
- [6] S. M. Howdle, M. S. Watson, M. J. Whitaker, V. K. Popov, M. C. Davies, F. S. Mandel, J. D. Wang, K. M. Shakesheff, *Chem. Commun.* **2001**, 109.
- [7] a) A. I. Cooper, A. B. Holmes, *Adv. Mater.* **1999**, *11*, 1270. b) C. D. Wood, A. I. Cooper, *Macromolecules* **2001**, *34*, 5.
- [8] C. Shi, Z. Huang, S. Kilic, J. Xu, R. M. Enick, E. J. Beckman, A. J. Carr, R. E. Melendez, A. D. Hamilton, *Science* **1999**, *286*, 1540.
- [9] C. T. Lee, P. A. Psathas, K. P. Johnston, J. deGrazia, T. W. Randolph, *Langmuir* **1999**, *15*, 6781.
- [10] S. R. P. da Rocha, K. P. Johnston, *Langmuir* **2000**, *16*, 3690.
- [11] K. P. Johnston, *Curr. Opin. Colloid Interface Sci.* **2001**, *5*, 351.
- [12] K. A. Consani, R. D. Smith, *J. Supercrit. Fluids* **1990**, *3*, 51.
- [13] M. J. Clarke, K. L. Harrison, K. P. Johnston, S. M. Howdle, *J. Am. Chem. Soc.* **1997**, *119*, 6399.
- [14] G. B. Jacobson, C. T. Lee, K. P. Johnston, *J. Org. Chem.* **1999**, *64*, 1201.
- [15] G. B. Jacobson, C. T. Lee, K. P. Johnston, W. Tumas, *J. Am. Chem. Soc.* **1999**, *121*, 11902.
- [16] K. P. Johnston, K. L. Harrison, M. J. Clarke, S. M. Howdle, M. P. Heitz, F. V. Bright, C. Carlier, T. W. Randolph, *Science* **1996**, *271*, 624.
- [17] P. A. Psathas, S. R. P. da Rocha, C. T. Lee, K. P. Johnston, K. T. Lim, S. Webber, *Ind. Eng. Chem. Res.* **2000**, *39*, 2655.
- [18] T. Sarbu, T. Styraneec, E. J. Beckman, *Nature* **2000**, *405*, 165.

Pure Silica Zeolite Films as Low-*k* Dielectrics by Spin-On of Nanoparticle Suspensions**

By Zhengbao Wang, Anupam Mitra, Huanting Wang, Limin Huang, and Yushan Yan*

The semiconductor industry has begun to develop ultra low-*k* materials, with the objective to achieve dielectric constant (*k*) below 2.2 for the technology nodes below 130 nm.^[1–3] Nanoporous sol-gel silica and surfactant-templated mesoporous silica have been studied as a potential candidates for ultra low-*k* materials.^[4–9] However, they have critical issues such as low mechanical strength, low thermal conductivity, wide pore size distribution (i.e., sol-gel silica), and moisture sensitivity.^[2,3] On the other hand, pure silica zeolite (silicalite) films

made by in-situ crystallization^[10] have several advantages as low-*k* materials, such as excellent mechanical strength (e.g., 30–40 GPa modulus of elasticity), good heat conductivity, hydrophobicity, and uniform molecular pores (e.g., 5.5 Å for silicalite). Unfortunately, their *k* value is relatively high (*k* = 2.7), and the hydrothermal synthesis procedure used is also of concern to semiconductor manufacturers.

Studies have shown that the *k* value of silicalite films could be reduced to the 1.8–2.1 range by spin-on of monodisperse silicalite nanocrystals.^[10,11] However, the spin-on films of monodisperse silicalite nanocrystals do not sinter well and have poor mechanical strength compared to in-situ crystallized-silicalite-films. Microwave treatment, an unpopular process with the semiconductor manufacturers, can be used to successfully increase the mechanical strength of the spin-on silicalite films although a slight increase in *k* value occurs simultaneously.^[10,11]

Recently, we have demonstrated^[12] the formation of porous zeolite films with surface patterns such as knotted-rope web and wrinkled honeycomb by convection-assisted dynamic self-assembly of zeolite nanoparticle suspensions. The nanoparticle suspension (containing nanoslabs and nanocrystals)^[12–15] offered unusual characteristics with potential applicability in microelectronic devices. In this communication, we report for the first time, the preparation of ultra low-*k* zeolite films with high mechanical strength by a simple spin-on process of a zeolite nanoparticle suspension followed by calcination (or baking) at 450 °C. Compared with the previously reported in-situ crystallization process, the spin-on process described in this study is simple and compatible with the requirements of the semiconductor manufacturers and therefore represents a significant step towards the integration of zeolite materials into microelectronic devices.

The deposition process for pure silica zeolite films is illustrated in Figure 1. First, a zeolite silicalite nanoparticle suspension with a range of particle sizes was synthesized hydrothermally

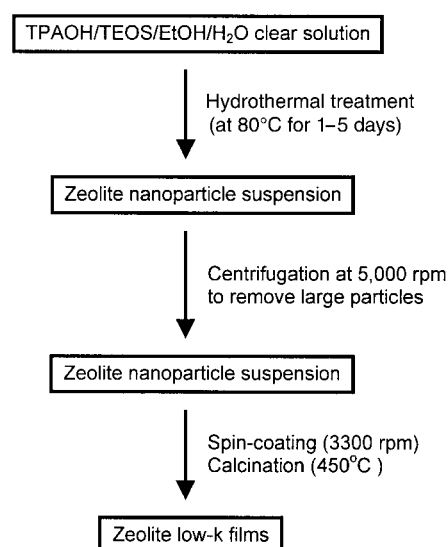


Fig. 1. Flowchart of the formation procedure of spin-on silicalite films using nanoparticle suspensions.

[*] Prof. Y. Yan, Dr. Z. B. Wang, Dr. A. Mitra, Dr. H. T. Wang, Dr. L. M. Huang
Department of Chemical and Environmental Engineering
University of California
Riverside, CA 92521 (USA)
E-mail: yushan.yan@ucr.edu

[**] This work was supported by Honeywell International, UC-SMART, UC-TSR&TP, UC-EI, EPA/NSF, and CE-CERT.